

Numerical Simulation of Bridge Deck Slab under High Cycle Moving Load

鉄筋コンクリート道路橋床版の輪荷重走行試験の再現解析

ADDISU BONGER^{*1}, RANKOTH CHAMILA^{*1}, HIROO SHINOZAKI^{*1}, WATARU SASAKI^{*1}

アデイス ボンガー, ランコス チャミラ, 篠崎 裕生, 佐々木 亘

This paper investigates the performance of precast prestressed concrete (PCaPC) deck slabs in steel plate girder bridges subjected to high-cycle fatigue under dry and wet conditions, using three-dimensional nonlinear finite element analysis referring to a past experimental program. The numerical simulation focused on the deflection, crack network development, failure mode, disintegrations of concrete, water leakage and stress level in reinforcing bar, and verify its findings by comparing with experimental data. Moreover, the simulation conducted in this study suggests the potential influence of liquid water pressure inside cracks and disintegrations of concrete in the specimen caused by the accumulation of cyclic liquid water pressure rise. This effect is analyzed without experimental verification, as it is hard to measure experimentally. The simulation results successfully reproduce the experiment, which indicates the credibility of the simulation.

Keywords: PCaPC slab, Fatigue loading, Simulation, Effect of water

本報では、乾燥および湿潤条件における繰り返し輪荷重作用下のプレキャストプレストレスト床版の耐荷性状を、コンクリートの空隙構造と水の影響を考慮できる三次元非線形有限要素解析を用いて再現した。解析の信頼性は、床版の変形、ひび割れの進展、破壊モード、漏水の状況、鉄筋の応力レベルなどを実験結果と比較することにより検証した。湿潤条件下における数値シミュレーションの結果、ひび割れ内部での周期的な液圧の変化と荷重増加にともなうその液圧の上昇がコンクリートの損傷を増大させていることが示された。このような液圧による影響を実験的に測定することは困難であるが、実験の破壊性状がシミュレーションと一致していることから、ひび割れ内部の液圧の変化が破壊の一要因であると考えられる。今回のシミュレーション結果は実験を良く再現できており、本解析手法は破壊メカニズムの解明に役立つものと考えられる。

キーワード: プレキャスト PC 床版, 輪荷重走行試験, 三次元非線形 FEM 解析, 水の影響

1. Introduction

Fatigue analysis and lifetime evaluation are important in design proposals to assure the safety and reliability of bridge deck slabs. With the powerful advancement in computer simulation technology and accumulation of past valuable experimental investigations, the mechanism of fatigue behavior and the prediction of lifetime for bridge deck slabs are becoming clearer and more accurate than before. In some previous studies, the fatigue behavior of RC bridge deck slabs is experimentally investigated and analytically simulated with full three-dimensional nonlinear finite

^{*1} Research & Development Institute, Technology Development Promotion Department

element analysis and water is found to cause a dramatic reduction in fatigue life of bridge deck slabs¹⁾.

This study focuses on the numerical simulation of a PCaPC (precast prestressed concrete) slab under running wheel load utilizing the data of a previous experimental program. Experimental results are reported in detail in references 2), 3). The simulation employs a multi-scale integrated nonlinear structural FEM system for RC structures. The objective of this paper is to clarify the behavior of the PCaPC slab under the running wheel load, which is challenging to study experimentally. Especially, the variable liquid water pressure inside cracks and disintegrations of concrete caused by the accumulation of cyclic liquid water pressure rise. Moreover, the numerical simulation investigates the deflection, the crack network development, failure mode, disintegrations of concrete, water leakage and stress level in the reinforcing bar and verifies its findings referring to the experimental data.

2. Experimental data

2.1 Basic specimen information

The PCaPC slab subjected to moving wheel-type loads described in reference 2) is used for the purpose of verification. The test specimen is shown in Fig. 1(a). The dimensions of the specimen are $8.45 \text{ m} \times 4.00 \text{ m}$ with a thickness of 220 mm and consists of four precast pre-tensioned slab panels connected by three joints (Fig. 1(b)). The panels are pretensioned in transverse direction using PC strands with a prestressing force of 144 kN. The joints are reinforced with trunc-head re-bars (Fig. 1(c)).

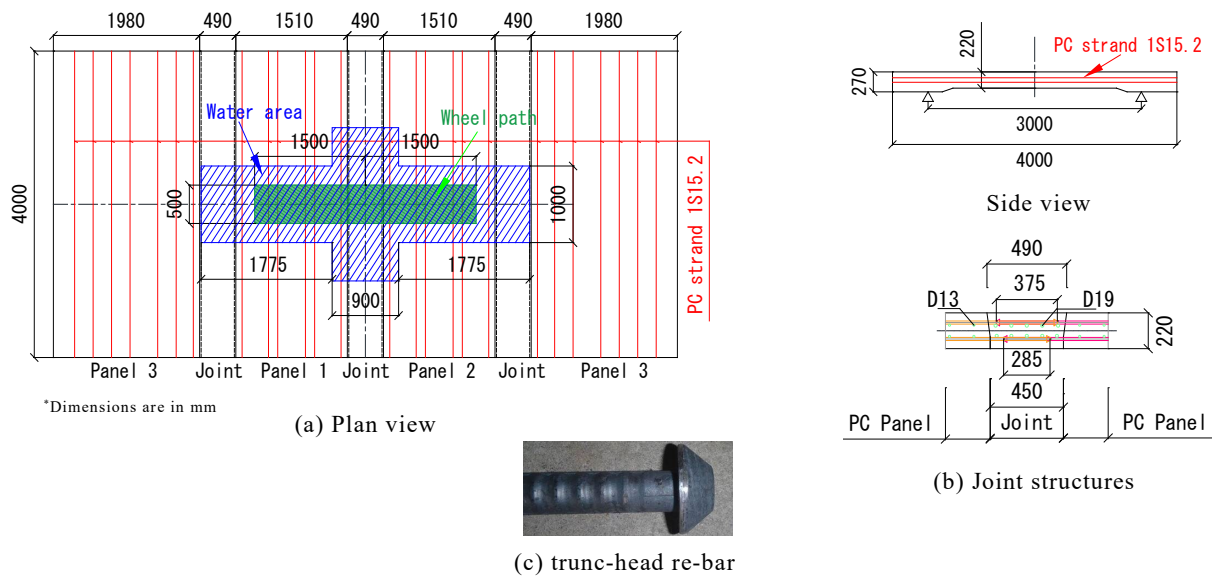


Fig. 1. Dimensions of the studied PCaPC slab

2.2 Material properties

Table 1 and Table 2 present the material properties of concrete and reinforcing bars. PC strand has a yield strength of 204 kN, a tensile strength of 240 kN, a cross-sectional area of 138.7 mm^2 , a rupture strain of 3.5%, and a Young's modulus of 200,000 MPa.

Table 1. Properties of concrete in the specimen

	Compressive strength (MPa)	Tensile strength (MPa)	Elastic modulus (MPa)
PCaPC slabs	90.0	4.2	38,100
Joints	52.5	3.28	30,500

Table 2. Properties of reinforcing bars in the specimen

Nominal diameter	Yield strength (MPa)	Tensile strength (MPa)	Young's modulus (MPa)
D19	376	575	191,000
D13	391	589	192,000

2.3 Wheel-type moving load

Table 3 shows the load pattern used in the experiment. The wheel loads are applied under both dry and wet conditions. For wet conditions, water is applied to the top of the slab in the blue area shown in **Fig. 1(a)**. The wheel travels along the wheel path indicated by the green area in **Fig. 1(a)**. Each cycle involves the wheel moving 3 meters from one end to the other at a speed of 5.4 km/hr. Static loading tests were conducted at intervals of 2,000, 10,000, 20,000, 40,000, and every 80,000 loading cycles to measure the deck slab deflection and various strains.

Table 3. Wheel load patterns under dry and wet conditions

	Load steps	Wheel load (kN)	Cycles	Cumulative cycles	Loading condition
Load patterns up to a service life of 121 years	1	180	100	100	dry
	2	180	50,000	50,100	dry
		180	4,000	54,100	wet
	3	200	220,000	274,100	dry
		200	40,000	314,100	wet
Load patterns up to destruction	4	240	40,000	354,100	wet
	5	280	40,000	394,100	wet
	6	320	40,000	434,100	wet
	7	360	40,000	474,100	wet
	8	400	40,000	514,100	wet
	9	440	40,000	554,100	wet
	10	480	Up to destruction		wet

3. Scheme of numerical analysis and modeling

3.1 Methodology of multi-scale simulations

The analytical studies presented in this paper are based on a multi-scale integrated nonlinear structural FEM calculation system for RC structures named COM3⁴⁾. In fatigue analysis, a single finite element consists of two parts, which represents the solid skeleton (SKLT) and the pore medium (PORE). This two-phase concrete-water interaction composite concept has been widely applied to fatigue life assessment of RC slabs⁵⁾. The solid skeleton can reproduce the three-dimensional dynamic nonlinear responses of RC structures based on the path-dependent constitutive laws for compression, tension, and shear⁴⁾ and incorporate the effects of cyclic loads such as fatigue actions on concrete with time-dependent models⁶⁾. **Fig. 2** shows the constitutive law of concrete under high cycle fatigue in compression, tension and shear.

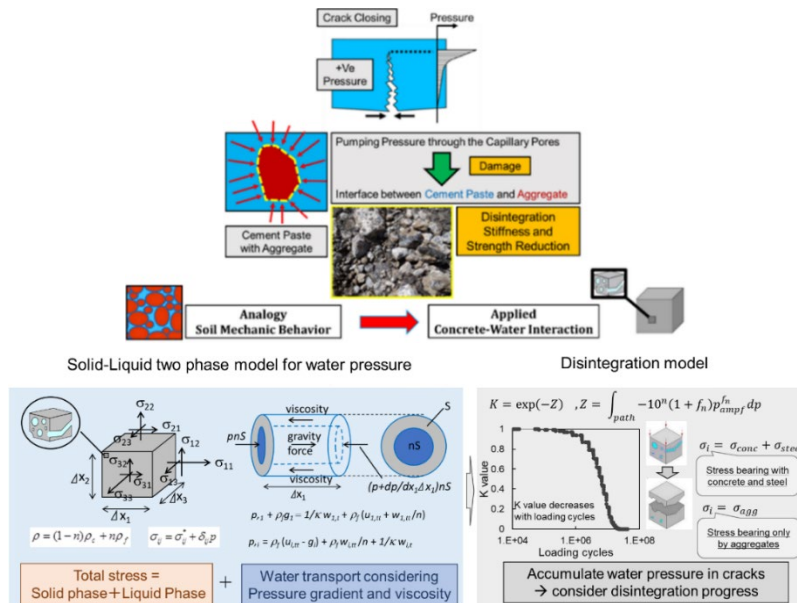
During repetitive loading, not only the progresses of plastic deformation of concrete, but also the development of micro cracks inside the concrete causes the elastic stiffness to decrease gradually. This behavior is incorporated into the fracture parameters in the basic constitutive law of compression, as shown in compression part of **Fig. 2**. $\sigma = E_o K_c \varepsilon$ is the basic constitutive equation to express the elasto-plastic and fracturing. σ is the total stress of concrete skeleton, E_o is initial stiffness, K_c is fracture parameter in compression considering time dependent plasticity and fracturing and cyclic fatigue damage, ε is total strain, ε_e is elastic strain, and ε_p is plastic strain. λ is the term expressing fatigue damage accumulation with incremental elasticity and is formulated with fracture potential F_k , R is a non-dimensional factor representing the amplitude, g is high cycle fatigue parameter, K in **Fig. 2** is fracture parameter, and K_m is micro cracks evolution parameter.

The decrease in stiffness due to the bond fatigue between reinforcing bars and concrete is reflected in the analysis as damage on the tension side (tension part of **Fig. 2**). K_T is tensile fracturing parameter, F is time dependent fracturing, H is instantaneous fracture, and G is fracture damage induced by high cycle load repetitions.

On the other hand, for the shear stress transfer model along a concrete crack surface, a micro-damage term is introduced that reduces the shear function according to the number of repetitions. In normal concrete, the crack surface is rough due to aggregate interlock. This roughness is smoothed due to repetitive loading from opening and closing of cracks, and the shear transfer between crack's surfaces is reduced gradually during loading cycles. The equations under shear is shown in **Fig. 2**, where τ is shear transfer through cracks under high cycle load, τ_0 is shear stress calculated by the referential contact density function. w is crack width and δ is crack slip. X is fatigue modification factor which is considered accumulation of shear deformation during load cycles.

	Compression	Tension	Shear
Core Concrete Models			
Enhanced Model For High Cycle Fatigue	<p>Fracture parameter K_c considers time dependent plasticity & fracturing and cyclic fatigue damage</p> $dK_c = \frac{\partial K_c}{\partial t} dt + \frac{\partial K_c}{\partial \epsilon_e} d\epsilon_e$ <p>Time Dependency Cyclic Fatigue</p> $\frac{\partial K_c}{\partial \epsilon_e} = \lambda \sim \text{when } F_k > 0$ $\frac{\partial K_c}{\partial \epsilon_e} = -\frac{\partial F_k}{\partial \epsilon_e} / \frac{\partial F_k}{\partial K_m} + \lambda \sim \text{when } F_k = 0$ $\lambda = K^3 \cdot (1 - K^4) \cdot g \cdot R$	<p>Fracture parameter K_T considers time dependent fracturing and cyclic fatigue damage</p> $dK_T = Fdt + Gd\epsilon_e + Hd\epsilon_e$ <p>Fdt: time dependent fracturing $Gd\epsilon_e$: cyclic fatigue damage</p>	<p>Accumulated path function X reduce shear associated with cyclic fatigue damage</p> $\tau = X \cdot \tau_0(\delta, w)$ <p>Function Original Model</p> $X = 1 - \frac{1}{10} \log_{10} \left\{ 1 + \int \left d \left(\frac{\delta}{w} \right) \right \right\}$ <p>≥ 0.1</p>
Physical Meaning	Decrease of Stiffness and Plasticity Accumulation by Continuous Fracturing Concrete	Decrease of Tension Stiffness by Bond Fatigue	Decrease of Shear Transfer Normal to Crack by Continuous Deterioration of Rough Crack Surface

Fig. 2. Constitutive laws of cracked concrete for high cycle fatigue^{4),6)}



(a) Solid-liquid two phase model for concrete (b) Disintegration progress model

Fig. 3. Solid-liquid two phase model for concrete and disintegration progress model^{5),7)}

The solid-liquid two-phase model considers the variable liquid water pressure inside cracks⁵⁾ (**Fig. 3(a)**). During fatigue loading cycles, the pore water pressure increases until it reaches the fatigue tensile limit of the interface between the cement binder and aggregates. The interface is damaged due this increment of local pore water pressure, which ultimately leads to disintegration of the aggregates and cement binder. The total stresses of concrete skeleton and pore water (σ_{ij}) is a simple summation of the skeleton stress (σ_{ij}^*) originated from particle contacts and the isotropic pore water pressure (p). ρ is total density of saturated concrete, ρ_c is density of concrete skeleton, ρ_f is density of pore water, and n in **Fig. 3(a)** is defined as the pore volume ratio. The dynamic equilibrium equation of fluid is based on Biot's theory, where the generalized dynamic equilibrium equation for each axis is also shown in **Fig. 3(a)**. Here, the motion of pore water is defined by the relative displacement from the solid particle. The movement of pore water particle denoted by U_i is expressed by the averaged displacement of the skeleton u_i and the substantial relative displacement of pore water phase w_i .

Fig. 3(b) shows disintegrations of concrete caused by the accumulation of cyclic liquid water pressure rise⁷⁾. In **Fig. 3(b)**, σ_i is the total compressive stress of a disintegrated reinforce concrete consists of three stress components: those of concrete (σ_{con}), reinforcement bars (σ_{steel}), and aggregates (σ_{agg}). The expression Z , express the overall stresses of the disintegrated reinforce concrete (the accumulated concrete damage in the micro-structure), n and f_n in **Fig. 3(b)** are coefficients related to the intersection and slope of the S-N diagrams (S is defined as the value of shear amplitude divided by static shear capacity and N is the cycle count at failure), where S-N diagram's coefficients equal to 2.0, 0.4, respectively. p_{ampl} is pore water pressure amplitude. As the disintegration progresses due to the increase in the local pressure at aggregates interface, the K (erosion factor) value in **Fig. 3(b)** decreases until full disintegration occurs ($K = 0$). Here, the total compressive force is only carried by the aggregates assembly by volumetric contraction similar to the analogy of soil particles in the geotechnical field. The stiffness of the aggregates assembly without cement binder is estimated to be 1/100 of the normal concrete. Finally, when concrete reaches full disintegration, slab loses its stability and fails. With the implementation of these models, it is possible to simulate the fatigue behavior of concrete structures in both dry and wet environments.

3.2 Simulation model

Fig. 4(a) shows the simulation model which utilizes three-dimensional SKLT and PORE elements. SKLT defines the constituent for solid skeleton and PORE defines pore water relative displacement. The slab model is discretized in the X-Y plane with a mesh size of 225×125 mm and divided into five elements in the thickness direction. Even though there were three joints in the test specimen, the damage was mainly observed in the slab panel. Therefore, modeling of the joint was done only by accurately representing the actual steel reinforcement in the joints and assigning appropriate material properties to the joint concrete. No special elements were used to model the interface between the slab panels and the joints.

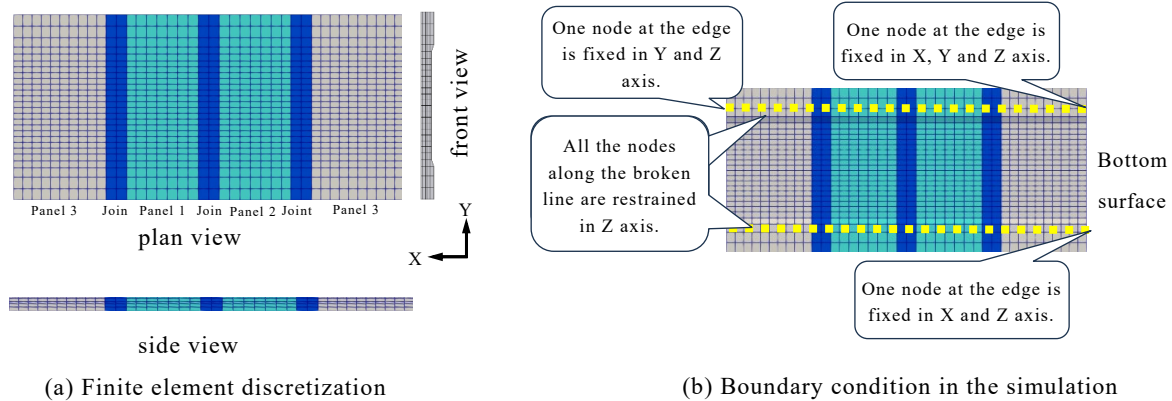


Fig. 4. Simulation model

Material properties in the simulation assigned according to the experimental program as shown in Section 2.2. The PCaPC slab was subjected to a running wheel load that follows experimental program as shown in Table 3. According to Japan's Specifications for Highway Bridges – Part III, the wheel load dimensions corresponds to tire contact areas are 250 mm and 500 mm⁸⁾. However, in the numerical simulation in this study, the wheel load dimensions were adjusted to 225 mm (x-direction) and 500 mm (y-direction). This modification was made to ensure mesh compatibility in accounting for the joint width and the length of the wheel path. The applied boundary conditions are shown in Fig. 4(b).

4. Simulation results

4.1 Deflection

4.1.1 Deflection at a standard load of 180 kN at 1st round

Before the wheel load running test, a static wheel load (180 kN) was applied in dry conditions at the center of the slab to obtain the maximum mid-span deflection. Deflections were measured on the bottom surface of the slab. The deflection in the experiment and in the simulation are compared as shown in Fig. 5. Fig. 5(a) shows the deflection profile along the centerline of the slab in the longitudinal direction when the wheel load is at the center of the slab. Fig. 5(b) shows the deflection profile along the centerline of the slab in the lateral direction when the wheel load is at the center of the slab. The deflection curves calculated by the analysis are almost consistent with the experimental results.

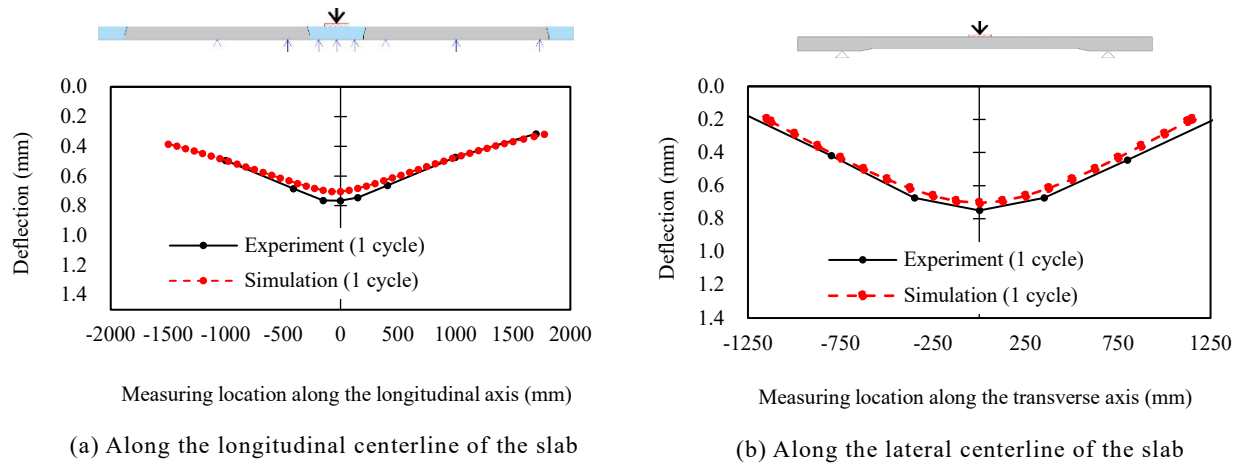


Fig. 5. Deflection profiles at 1 cycle with 180 kN static wheel load (static response)

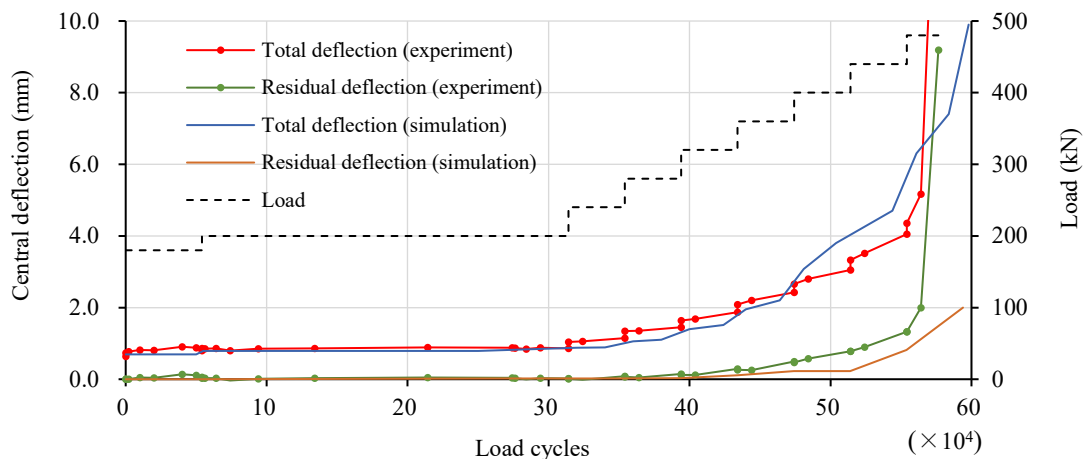


Fig. 6. Change in deflection at center of the deck slab with number of cycles (dynamic response)

4.1.2 Total live load and residual deflection

Fig. 6 shows the progress of mid-span deflection in the numerical simulation and in the experiment. The deflection response in the numerical simulation shows a similar tendency to that of the total deflection and the residual deflection in the experiment. 1 to 314,100 cycles, the deflection in both the numerical simulation and the experiment was small, with no significant increase in mid-span deflection. However, when the wheel load is increasing in wet condition (after 314,100 cycles), the total and residual mid-span deflection in the center of the slab increases rapidly. In the last load step (480 kN wheel load), the slab deteriorates rapidly, leading to punching shear failure in the numerical simulation and in the experiment.

4.2 Cracking pattern and failure mode

The experimental crack pattern on the bottom surface and the principal strain contours in the simulation are compared in **Fig. 7(a)**. Higher principal strain regions imply wider or numerous cracks. For verification, the principal strain was compared with the cracking pattern. The elastic cracking strains in the PCaPC slab and in the joint are 110μ and 108μ respectively, which can be calculated by dividing the tensile strength of the concrete by the elastic modulus. In the simulation, the cracking process of the slab in dry condition was relatively slow and started with cracks at the bottom surface. However, in wet conditions, cracks progress more quickly on the bottom surface and inside of the slab. The ultimate failure mode in the simulation was punching shear failure, as shown in **Fig. 7(b)**, which was similar to the experimental observations. The extent of degradation in different slab sections was evaluated through simulation and validated against experimental data, as illustrated in **Fig. 7(c)**. The results indicate severe slab deterioration, characterized by widespread cracking and loss of structural integrity.

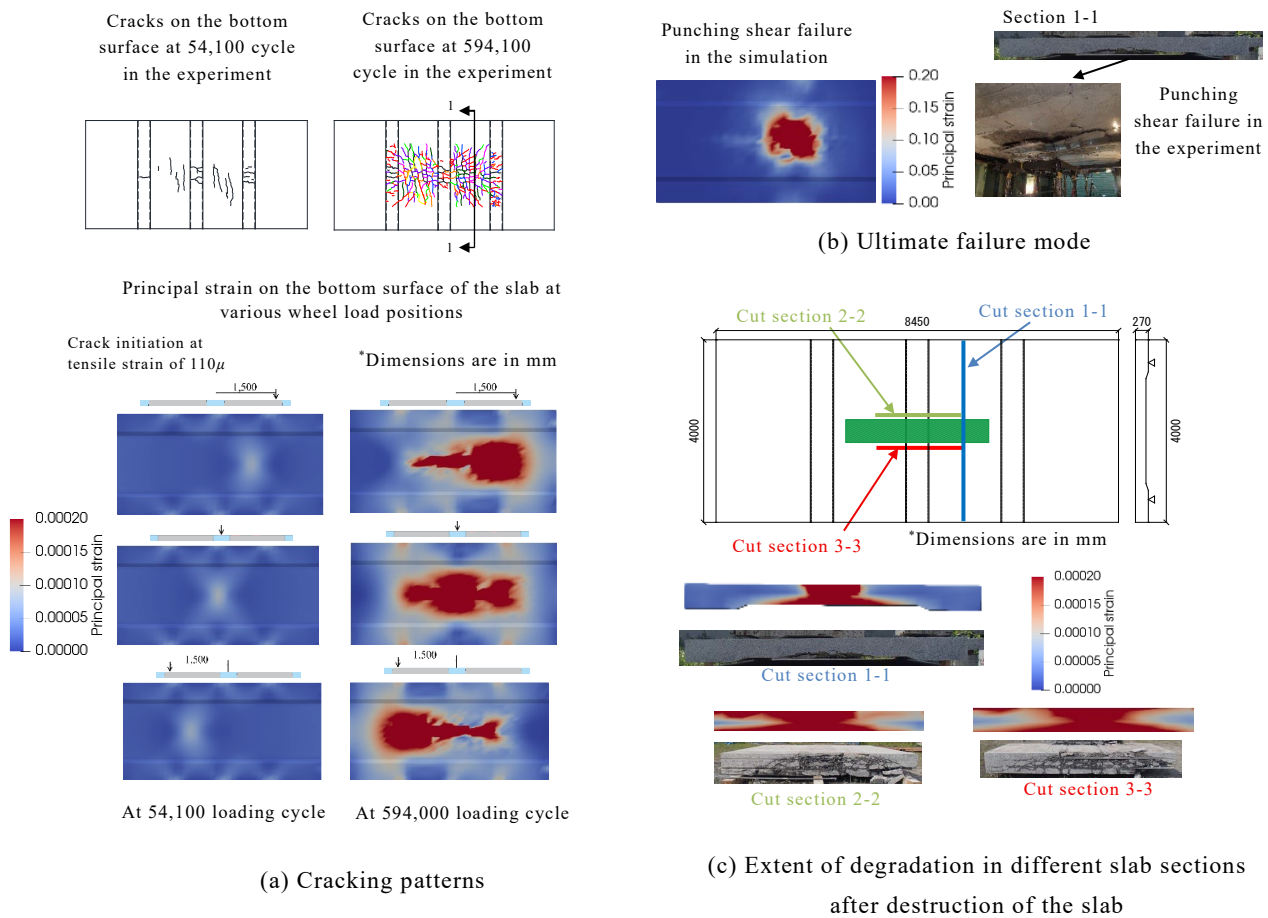


Fig. 7. Cracking pattern and failure mode

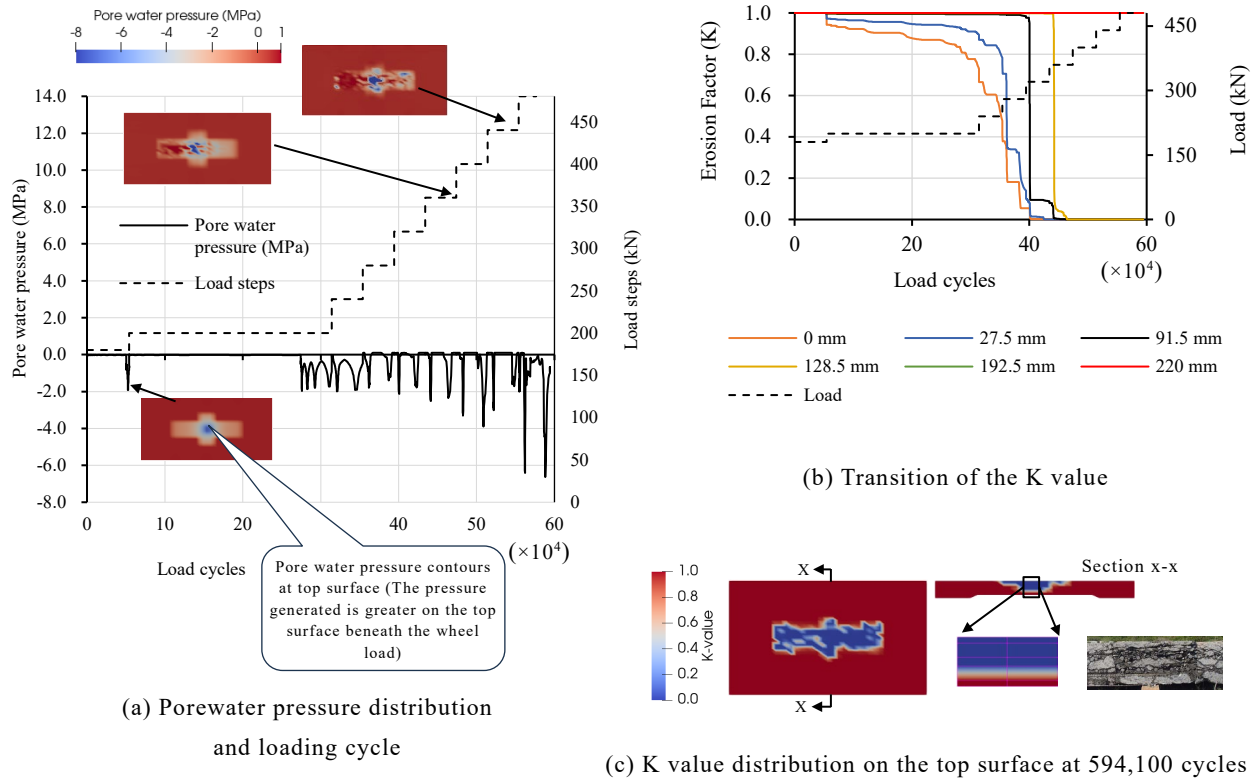


Fig. 8. Pore-water pressure and disintegration of slab

4.3 Pore-water pressure and disintegration of the slab

As discussed in Section 3.1, fatigue failure in wet conditions is influenced by the amplitude of pore-water pressure. Fig. 8(a) shows the relation between porewater pressure distribution and loading cycles. The pore-water pressure rises as the number of load cycles increases. The rise in pore-water pressure primarily takes place at the location of the wheel load. Additionally, the pressure generated is greater on the top surface beneath the wheel load. Infiltrated water is discharged through cracks and pore networks at the bottom surface, leading to decreased water retention and reduced pore-water pressure in this region.

Fig. 8(b) illustrates the transition of the erosion factor (K) value during fatigue simulation at the slab center for different slab thicknesses. As mentioned in Section 3.1, K is an index that reflects the disintegration degree: $K = 1$ indicates that the slab region is sound and $K = 0$ indicates full disintegration. At the top surface, the initial K value is 1.0, gradually decreases with the accumulation of the cyclic water pressure. The disintegration degree is particularly severe along the vehicle's wheel position. However, the K value at the bottom surface remains constant at 1.0 throughout all loading cycles. A previous study⁹⁾ identified $K = 0.1$ is indicative of concrete disintegration. From the simulation in this study, disintegration occurs after 384,000 loading cycles. Fig. 8(c) presents the distribution of K values on the top surface of the slabs at 594,100 loading cycles.

4.4 Water leakage at the joint interface

In the simulation, principal strains at the joint interface were observed at various points in slab thickness direction (Fig. 9) to determine the loading cycle at which a penetrating-crack developed. It is assumed that water leakage initiates once a penetrating-crack has developed. The elastic cracking strain at the joint is 108μ . In the simulation, penetrating-cracks in the floor slab were observed to develop at approximately 440,000 loading cycles under a wheel load of 360 kN, marking the onset of water leakage at the bottom surface. In the experiment, water leakage was observed to initiate at approximately 400,000 loading cycles under a wheel load of 360 kN, which is close to the simulation-based estimation.

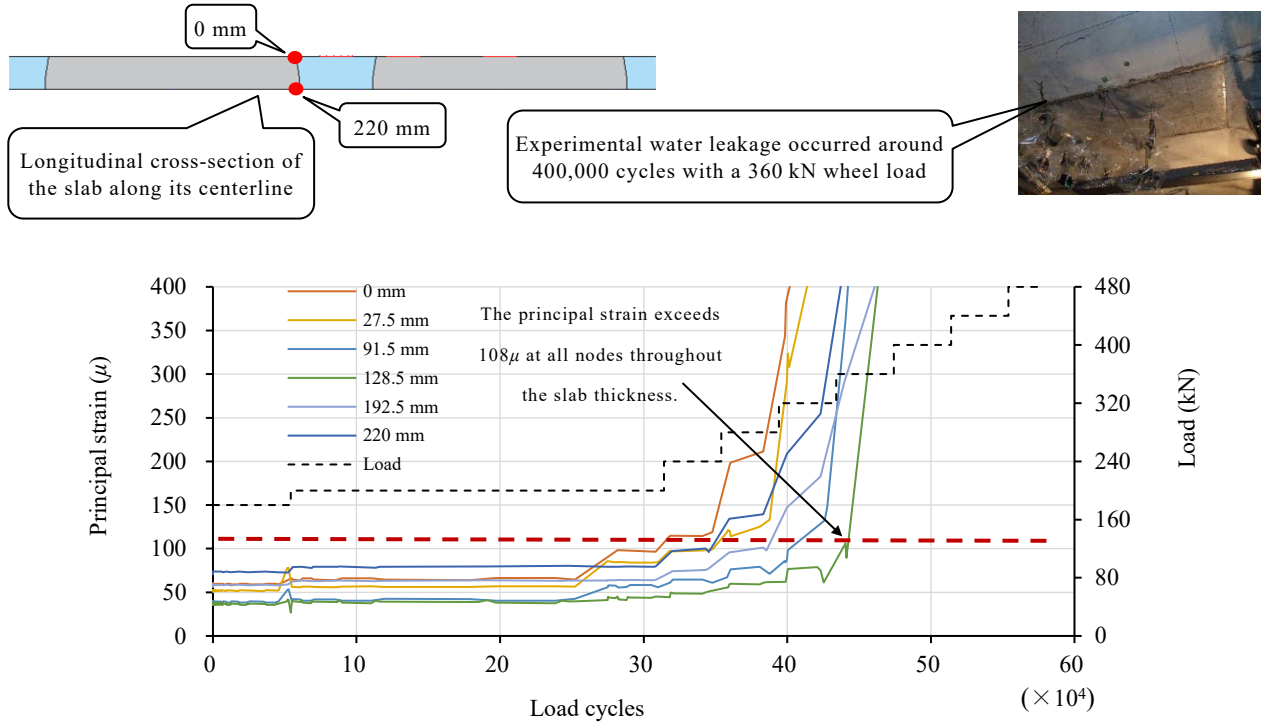


Fig. 9. Principal strains at the joint interface in the longitudinal cross-section of the slab along its centerline

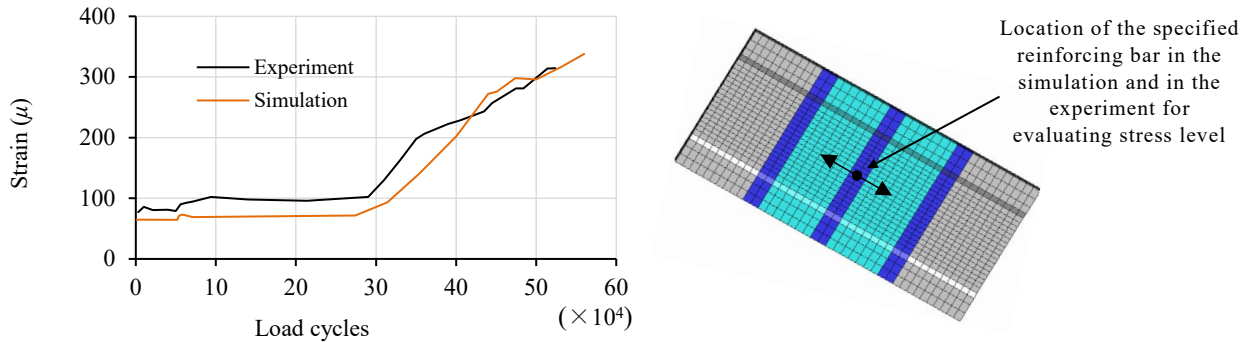


Fig. 10. Number of load cycles and tensile strain in the bottom longitudinal reinforcement at the slab's center zone

4.5 Stress level in the reinforcing bars

Fig. 10 presents the computational assessment of stress level in the bottom longitudinal reinforcing bar located in the central part of the slab (27.5 mm above from the bottom surface). The reinforcing bar strain shown in Fig. 10 represents the live load strain, which is calculated by subtracting the residual reinforcing bar strain from the total reinforcing bar strain at a specific loading cycle. The simulation showed that the reinforcing bar strain did not increase approximately until 300,000 cycles, a behavior similar to the experimental findings. After surpassing 300,000 cycles, the reinforcing bar strain progressively increased with additional loading cycles. This was also verified by experimental results.

5. Conclusions

In this paper, a fatigue analysis study was conducted using a full-scale PCaPC slab with trunc-head joint using a multi-scale integrated analytical system. The fatigue load was applied with different loading steps under dry and wet

conditions. The deflections, cracking patterns, failure mode, disintegration of concrete and stress level in reinforcing bar are numerically investigated. The simulation results are compared with the experiment. The progress of mid-span deflection and punching shear failure mode under a high cycle moving load are successfully replicated by simulation. The crack patterns on the bottom surface, analyzed computationally using principal strain, closely resemble those observed in the experimental results. In the simulation, the beginning of water leakage was assessed based on forming of a penetrating crack and was close to the experimental behavior. In the simulation, the reinforcing bars did not reach the yield strain under fatigue loading. This was also verified by experimental results, which indicates the credibility of the simulation. From the simulation results, it is inferred that damage to the PCaPC slab was accelerated by high pore water pressure in the cracks when wet, leading to its collapse. This simulation technique might be employed to assess the remaining fatigue life of an existing bridge by utilizing monitoring data.

References

- 1) Fujiyama C, Kobayashi K, Zhan J, and Maekawa K: “Fatigue life simulation of RC bridge slab with initial defects under water”, The 12th East Asia-Pacific Conference on Structural Engineering and Construction, Procedia Engineering 14, pp.1897-1904, 2011
- 2) 三加崇, 有川直貴, 鈴鹿良和, 中積健一: 端部拡張鉄筋を用いたプレキャスト PC 床版継手の開発, プレストレストコンクリート工学会 第 26 回シンポジウム論文集, pp.199-204, 2017.10
- 3) 三加崇, 有川直貴, 鈴鹿良和, 篠崎裕生: Trunc-head を用いたプレキャスト PC 床版継手の開発, 三井住友建設技術研究開発報告 第 15 号, pp.23-26, 2017
- 4) Maekawa K, Pimanmas A, and Okamura H: “Nonlinear mechanics of reinforced concrete”, London: Spon Press; 2003
- 5) Maekawa K and Fujiyama C: “Rate-dependent model of structural concrete incorporating kinematics of ambient water subjected to high-cycle loads”, Engineering Computations, 30(6), pp.825-841, 2013
- 6) Maekawa K, Gebreyouhannes E, Mishima T and An X: “Three-dimensional fatigue simulation of RC slabs under traveling wheel-type loads”, Journal of Advanced Concrete Technology; 4(3), pp.445-457, 2006
- 7) Maekawa K, Ishida T, Chijiwa N and Fujiyama C: “Multiscale coupled-hygro-mechanistic approach to the life-cycle performance assessment of structural concrete”, ASCE, A4014003, pp.1-9, 2015
- 8) Japan Road Association, Specification for Highway Bridges-Part III Concrete Bridges, 2012
- 9) 古川智也, 高橋佑弥: 道路橋鉄筋コンクリート床版上面における土砂化発生特徴に関する数値解析的検討, コンクリート工学年次論文集, Vol.43, No.2, 2021